International Journal of Innovative Research and Advanced Studies (IJIRAS)
Volume 6 Issue 5, May 2019

ISSN: 2394-4404

Performance Of NCC- And SCC-DFTB Methods For Geometries And Energies Of Crystalline Molecular Gyroscope

Dr. Anant Babu Marahatta

Lecturer, GEMS School, GEMS Institute for Higher Education, Department of Chemistry

Prof. Hirohiko Kono

Emeritus Professor, Tohoku University, Graduate School of Science, Department of Chemistry

Abstract: ***The density-functional based tight-binding (DFTB) approximation is as familiar as other theoretical methods due to its versatility and efficiency in quantum mechanical calculations and its fundamental formulation based on density functional theory (DFT). The two approaches of DFTB are based on the zeroth- and second- order expansion of the Kohn-Sham total energy in DFT with respect to charge density fluctuations, known as "non-self-consistent-charge DFTB" (NCC−DFTB) and "self-consistent-charge DFTB" (SCC−DFTB) respectively. We have applied both methods to the experimentally observed crystalline siloxaalkane molecular gyroscopes and examined their ability to predict crystal structures and rotational barriers for the rotator. Like in X-ray crystallography, both methods produced three stable structures α, β, and γ which are found consistent with the three X-ray structures A, B, and C [Setaka et al, 2007] respectively and estimated equal amount of free space available around the rotator. By scanning potential energy surface (PES) as a function of the dihedral angle between the phenylene ring and a surrounding spoke under periodic boundary condition (PBC), the three equilibrium structures α, β, and γ with the respective counter positions α', β', and γ' are confirmed by both methods. However, after introducing dispersion energy correction parameters, the NCC−DFTB reproduced only one feature similar to SCC−DFTB derived PES: the most stable structure β and its degenerate position β'. This failure is mostly due to avoiding charge interactions between atoms in NCC−DFTB formulation. Thus, along with the dispersion energy correction parameters, formulating and computing charge interactions between atoms (as in SCC−DFTB) is mandatory to address comparatively weaker hydrogen bonds and van der Waals interactions exist between the rotator and static framework (and surrounding molecules).***

Keywords: ***NCC− and SCC− DFTB methods, Molecular gyroscope, Dispersion energy correction, Optimization and rotational energy barrier***

I. INTRODUCTION

As a fundamental element of nanotechnology, the synthesized crystalline molecular gyroscopes with bridged π-electronic system as a rotator have been receiving much attention. They are expected to possess many interesting physicochemical properties. For example, a dipolar unit attached to the rotator can be reoriented by conserving its volume under the influence of external stimuli [Dominguez *et al*, 2002]. Setaka *et al* synthesized a molecular model having closed topology (chart 1a) with a large free space around the rotators and it is quite analogous to macroscopic gyroscope (chart 1b) used in internal navigation system. By an X-ray crystallography, they confirmed silicon-based crystalline molecule with phenylene rotator encased in three long siloxaalkane spokes and observed the facile and repeated rotation of the phenylene ring inside the case [Setaka *et al, 2007*] and called it as siloxaalkane molecular gyroscope. The X-ray structure of this molecule with three stable phenylene positions indicated by colored spheroids and the arrangement of the atoms in stator are shown in Figure 1, where the rotator, stator, and spin axis are encircled. By considering its gyroscopic design and potential application in nanotechnology, we decided to extend the theoretical methods to elucidate the experimentally observed crystal structures and facile phenylene rotation. The density-functional-based tight-

ISSN: 2394-4404

binding (DFTB) methods for electronic structure calculations [Kohn and Sham, 1965; Porezag *et al*, 1995; Seifert *et al*, 1996; Elstner *et al*, 2001; Aradi *et al*, 2007] became our choice as they are already known to achieve an accuracy typical of standard time-dependent density functional theory (DFT) at a low computational cost.

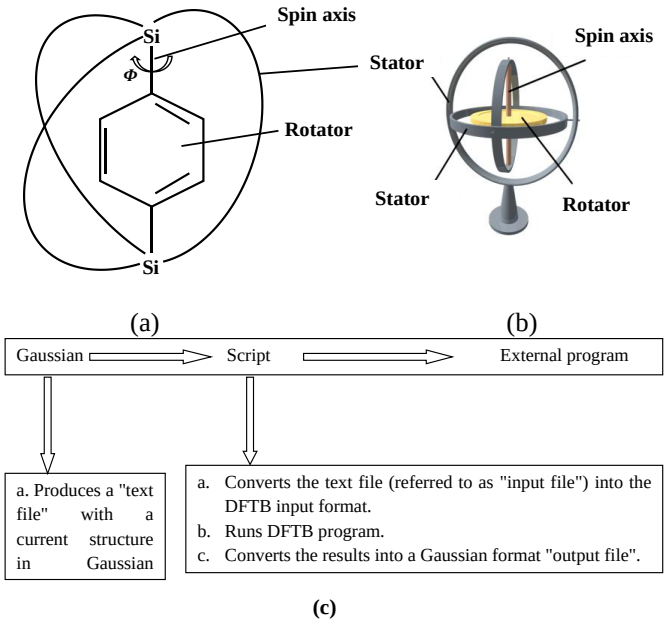

The DFTB method employs Slater−Kirkwood model [Elstner *et al*, 2001] in order to account the dispersion energy correction and implements the Slater−Koster files (SK−files) with a focus on solid state systems [Rauls *et al*, 1999; Koehler *et al*, 2001]. It has two different approaches: the zeroth-order expansion of the Kohn-Sham total energy in DFT with respect to charge density fluctuations is "non-self-consistent-charge DFTB" (NCC−DFTB) method [Seifert, 2007] and the second-order approach is equivalent to a "self-consistent-charge DFTB" (SCC−DFTB) [Elstner *et al*, 1998; Frauenheim *et al*, 2002]. The NCC-DFTB method is a traditional tight-binding method in which an eigenvalue of the Hamiltonian operator is a noniterative solution. It is very successful in nonpolar and homonuclear systems, such as carbon fullerene clusters [Zheng *et al*, 2005]. On the other hand, in the SCC−DFTB method, the charge distribution in a molecule, represented by point charges, is obtained in an iterative self-consistent manner by taking into account charge interactions between atoms. It thus enables one to cope with systems where the charge balance between atoms is crucial, as for instance in biomolecules and other heteroatomic molecular systems [Elstner *et al*, 2000]. As the self-consistent calculation of Mulliken charges is introduced in the *SCC* procedure and corresponding nuclear forces are derived, the SCC−DFTB with and without dispersion energy correction parameters under periodic boundary condition (hereafter, PBC) differs with similar types of NCC−DFTB in mathematical format. Due to this, the SCC−DFTB has been successfully applied to many complex molecular systems, where deficiencies within the NCC−DFTB approach become obvious. That is why, it is essential to examine the computing accuracy and performance of these two methods while applying them separately to experimentally observed crystalline molecular gyroscope shown in Figure 1. In our previously published research paper [Marahatta *et al*, 2012], we straight forward explained the theoretically predicted geometries and rotational dynamics of the crystalline molecular gyroscope rather than evaluating their computing abilities. So we decided to express our research work in another form. For this purpose, we have reproduced here few data sets and figures from our original publication [Marahatta *et al*, 2012].

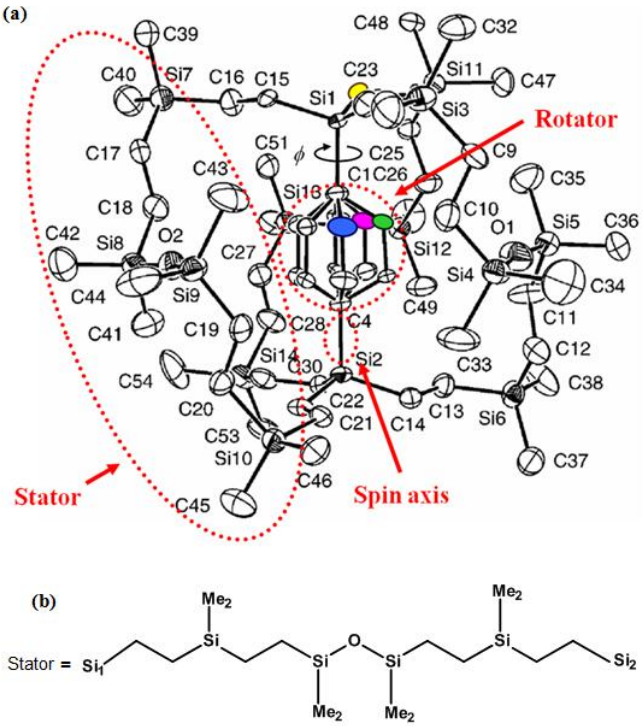

Figure 1: (a) An X-ray crystallography of the synthesized siloxaalkane molecular gyroscope. Three stable positions of the phenylene ring are clearly noticeable. Hydrogen atoms are omitted for clarity. (b) A schematic representation of the siloxaalkane stator. Si_1 and Si_2 represent two terminals of each siloxaalkane arm respectively. Me_2 stands for $(CH_3)_2$ group

This work is mainly aimed at evaluating the computing abilities of NCC− and SCC− DFTB methods under PBC with and without dispersion energy corrections. We have chosen two parameters: Geometries and Energies of siloxaalkane molecular gyroscope and examined the performance of these two methods. The structure of this paper is as follows. The computational methods we employed are outlined in section 2. The results and discussions are presented in section 3. A summary and conclusions are given in section 4.

II. COMPUTATIONAL METHODS

To optimize the geometry of molecular gyroscope, we took the initial atomic coordinates (trial structures) of three equilibrium structures A, B, and C directly from the X-ray crystallographic data and fully optimized them separately under the PBC by NCC− and SCC− DFTB methods while fixing the experimental unit cell parameters.

We calculated the rotational energy barrier experienced by the rotator, i.e., the electronic energy as a function of a particular dihedral angle between the phenylene ring and the reference plane of a siloxaalkane spoke. We selected C23 (shown by colored spheroid in Figure 1a) as one of the four atoms to define dihedral angle. While calculating the electronic energy, the dihedral angle must be fixed at certain value and other degrees of freedom must be fully relaxed to minimize the energy. This type of optimization cannot be carried out routinely in the DFTB+ program package. We, therefore, utilized the molecular geometry optimizer implemented in GAUSSIAN 03 [Frisch *et al*, 2004]. We called this optimizer by an external script and run the DFTB program via the Gaussian keyword "external". We refer to this methodology as "Gaussian-external" whose working steps are summarized in chart 1c. Additionally, we also applied dispersion energy parameters for addressing van der Waals interactions (Intra- and inter- molecular) under PBC. The detailed explanation is given elsewhere (Marahatta *et al*, 2012).

III. RESULTS AND DISCUSSIONS

A. OPTIMIZED GEOMETRIES

By using DFTB+ and GAUSSIAN 03 (i.e., the Gaussian external methodology) optimizers separately, we optimized all the three X-ray stable structures and confirmed that the converged structures and energies are same. It implies that the experimentally observed three equilibrium structures can also be located by theoretical methods. The phenylene dihedral angles for the three X-ray equilibrium structures are 0.78π, 0.55π, and 0.19π (modulo π), of which structures or dihedral angles are denoted by A, B, and C, respectively (Table 1). In the NCC−DFTB method, these angles are converged to 0.77π, 0.35π, and 0.05π and in the SCC-DFTB method, 0.77π, 0.35π, and 0.04π respectively. It indicates that both DFTB methods are equally valid to reproduce the experimentally observed equilibrium structures.

Methods	Structure **A**				Structure **B**				Structure **C**			
	Φ	θ	d_{CO}	E_{rel}	Φ	θ	d_{CO}	E_{rel}	Φ	θ	d_{CO}	E_{rel}
X-ray	0.78	0.90 0.96 0.94	3.9 4.5 4.6	—	0.55	0.90 0.96 0.94	3.9 4.3 5.1	—	0.19	0.90 0.96 0.94	3.9 4.3 5.1	—
DFTB:												
NCC	0.77	0.77 0.77 0.79	4.1 4.1 4.9	143	0.35	0.79 0.78 0.81	4.1 4.1 5.2	0	0.05	0.77 0.81 0.81	4.4 4.9 5.0	168
SCC	0.77	0.78 0.78 0.80	4.1 4.1 4.9	199	0.35	0.80 0.79 0.83	4.1 4.1 5.3	0	0.04	0.78 0.82 0.82	4.4 5.0 5.1	210
Gaussian external:												
NCC-DFTB	0.76	0.77 0.77 0.79	4.1 4.1 4.9	143	0.35	0.79 0.790. 81	4.1 4.1 5.2	0	0.05	0.77 0.81 0.81	4.4 5.1 5.1	168
SCC-DFTB	0.76	0.79 0.79 0.80	4.1 4.1 4.9	199	0.35	0.79 0.79 0.83	4.1 4.1 5.3	0	0.01	0.79 0.82 0.82	4.6 5.1 5.1	210

[a] *Φ = Phenylene dihedral angle (π); θ = Si−O−Si angle of each arm (π); d_{CO} = distance between the O atom of each siloxaalkane spoke and the nearest C atom of phenylene (Å); E_{rel} = relative energy to that of the structure B (cm^{-1}). The three data sets for one method correspond to three siloxaalkane spokes*

Table 1: Comparison between NCC−DFTB and SCC−DFTB optimized parameters of three different equilibrium structures

If we go through the measured Si−O−Si angles of each siloxaalkane spoke of each X-ray equilibrium structure listed in Table 1, they are found to be exactly equal. This is because each spoke acts as a static arm while rotating phenylene rotator inside the case. These angles are found to be slightly smaller in the NCC− and SCC− DFTB optimized geometries than in the X-ray geometries. However, this is fairly in good agreement if we consider the flexibility of the Si−O−Si linkage. The partial ionic and double bond characters of this linkage not only govern its strength but also contribute to exceptional conformational flexibility of the $-(Si-O)_x-$ chains and their segments [Richard *et al*, 2000]. In turn, these characteristics are directly responsible for the elasticity of the siloxaalkane arms. The Si−O−Si angles are found to be reproduced well in NCC− and SCC− DFTB optimized geometries.

The available space (free volume unit) exists inside the siloxaalkane spokes gives freedom to the rotating unit. Because of the flexibility of the spokes that causes them to squeeze inward, there is high chance of creating narrow space around the rotator, and hence increasing the intra-molecular interactions between rotator and stator, which ultimately causes hindered rotation. In other words, the rotator can only rotate smoothly if it experiences minimum rotational energy barrier. It clarifies that there is a direct relation between free volume unit and rotational energy barrier. That is why, it is essential to approximate the free volume unit around the rotator. In siloxaalkane molecular gyroscope, the free volume unit is the space exists between the O atom of each siloxaalkane arm and the nearest C atom of the phenylene ring (d_{CO}). The measured distances d_{CO} of all the three experimentally observed and theoretically converged geometries are tabulated (Table 1). The values d_{CO} of the optimized structures are in close agreement with the experimental values. These values are consistent in the NCC− and SCC− DFTB optimized geometries. Thus, the theoretically converged equilibrium structures also have enough free volume unit around the rotator like in X-ray observed structures.

The NCC−DFTB and SCC−DFTB optimized structures of type B in a unit cell are displayed in Figures 2a and 2b respectively where rotators are encircled. By comparing these two figures, one can reconfirm the above mentioned features for the optimized structures that the phenylene dihedral angle, the Si−O−Si bond angles of three siloxaalkane spokes and the free volume unit are well reproduced. Besides that the orientation and conformation of the methyl groups attached to the Si−O−Si part of the siloxaalkane spokes are also not noticeably different. Similarly, the optimized geometries of type B in a unit cell produced by NCC− and SCC− DFTB with Gaussian external method are shown in Figures 3a and 3b, respectively where rotators are encircled. The optimized geometries shown in Figure 2a and 2b are found to be quite analogous to the optimized geometries shown in Figure 3a and 3b, respectively. It reconfirms that both DFTB+ and Gaussian optimizers converge to energetically similar structures.

ISSN: 2394-4404

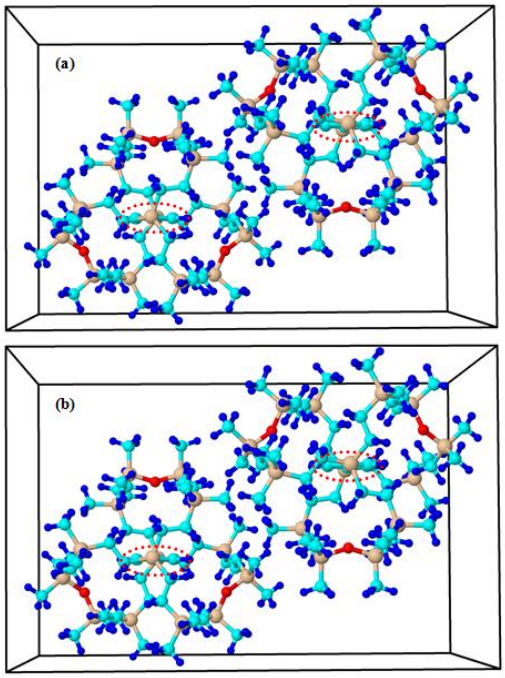

Figure 2: (a) NCC−DFTB and (b) SCC−DFTB optimized unit cell geometries for the most stable structure B viewed along the spin axis. The blue, cyan, red, and gray spheroids represent hydrogen, carbon, oxygen, and silicon atoms, respectively. The phenylene rings are encircled.

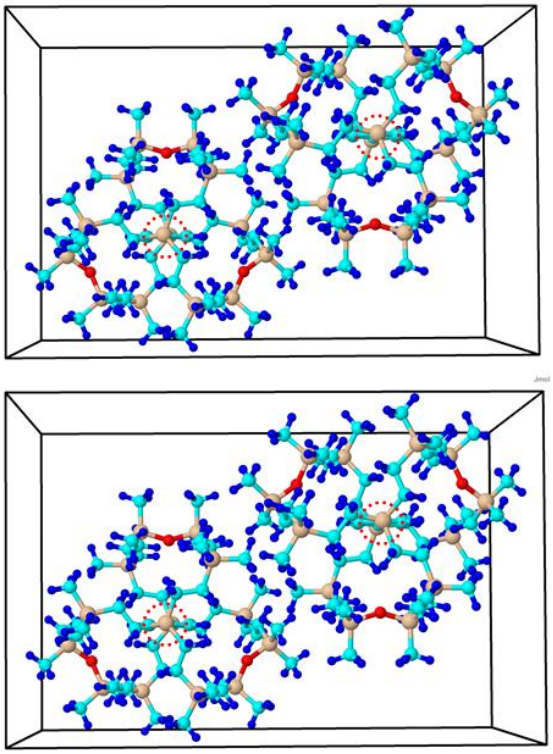

Figure 3: (a) NCC−DFTB + Gaussian external and (b) SCC−DFTB + Gaussian external optimized unit cell geometries for the most stable structure B viewed along the spin axis. The blue, cyan, red, and gray spheroids represent hydrogen, carbon, oxygen, and silicon atoms, respectively. The phenylene rings are encircled.

B. POTENTIAL ENERGY SURFACES

To scan the potential energy surface (PES) under PBC, we chose the most stable X-ray structure as a starting point (i.e. 0.55 π, X-ray position B) and rotated phenylene ring by 360˚ (2 π) in the increments of 2.0˚. The PESs for three different cases are plotted in Figure 4 against the dihedral angle up: NCC−DFTB without dispersion correction (brown dotted line); SCC−DFTB without dispersion correction (black dotted line); SCC−DFTB with dispersion correction (thick solid line). While scanning the PES with dispersion energy correction under PBC, we explicitly took previously optimized geometry from "SCC−DFTB under PBC" and computed the SCC−DFTB single point energies (SPE) with dispersion energy parameters.

Each PES displays three stable positions clearly upon 1 π phenylene rotation. They are denoted by *α*, *β*, and *γ* in Figure 4. The dihedral angles of the three minima in the NCC−DFTB case are 0.78π, 0.35π, and 0.01π, respectively, which are close to the corresponding values 0.78π, 0.55π, and 0.19π of the X-ray structures A, B, and C, as already shown in Table 1.These angles are also well reproduced by SCC−DFTB method with and without dispersion energy corrections. Each equilibrium structure has a degenerate position reached by 1 π flip as denoted by *α′*, *β′*, and *γ′*, respectively. The 1 π phenylene flipping is illustrated just above the potential wells in Figure 4. The dotted lines around the rotary phenylene unit represent the cage-like environment. In addition, each PES shows significantly low activation barriers for phenylene flipping. The activation energy E_a for the flipping from *β to γ* is ~ 280 cm^{-1} for the SCC−DFTB under PBC, while it increases to ~ 400 cm^{-1} while addressing dispersion energy corrections. This value is slightly smaller (~240 cm^{-1}) in the NCC−DFTB case under PBC.

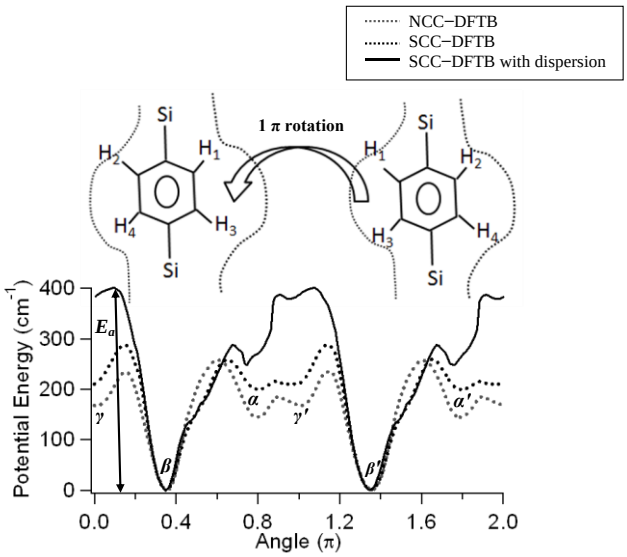

Figure 4: Potential energy as a function of the phenylene dihedral angle under the PBC. The brown dotted, black dotted, and thick solid lines denote the PESs obtained by the NCC−DFTB, SCC−DFTB, and SCC−DFTB with dispersion correction, respectively. The symbols α, β, and γ stand for three stable positions of the phenylene ring, and α′, β′, and γ′ represent their respective degenerate positions reached by 1 π

phenylene flip. The dotted lines around the phenylene rotator indicate the cage-like environment

We also scanned the PES by computationally less expensive NCC−DFTB method under PBC with dispersion energy corrections. For this, we explicitly took previously optimized geometry from "NCC−DFTB under PBC" and computed NCC−DFTB/SPE calculations with dispersion energy parameters. The PES is plotted along with the PES derived by SCC− DFTB/SPE method (Figure 5). One of the prominent features of both PESs is the reproduction of the most stable structure B, its dihedral angle β and its degenerate structure β' reached by 1 π flip. However, there is no any indication of appearing two more stable positions (α and γ) of the molecular gyroscope upon 1 π phenylene rotation on the PES derived by NCC−DFTB/SPE. The NCC−DFTB/SPE computed energy barrier seems slightly higher than that observed on the PES derived by SCC−DFTB/SPE. But this energy barrier is for direct 1 π flip from β to β' position as there are absence of α and γ' positions in between them. It is a very contrasting result produced by NCC−DFTB/SPE because the structure B at position β has to flip to position α then to γ' before reaching to β' as observed clearly in X-ray crystallography. It elucidates that the NCC−DFTB with dispersion energy parameters under PBC is unable to produce experimentally observed three stable structures. This inability is most probably due to not addressing charge interactions between atoms properly unlike in SCC−DFTB. Thus, while calculating electronic energy, the effect of van der Waals interactions exist between the phenylene rotator and the siloxaalkane spokes: intra-molecular interactions (and surrounding molecules: intermolecular interactions) can be addressed only by SCC−DFTB with dispersion energy parameters. It is a strong supporting evidence for the SCC−DFTB method to recommend it for addressing comparatively weaker hydrogen bonds and van der Waals interactions that exist in the molecular crystal. Therefore, the SCC−DFTB with dispersion energy corrections under PBC puts considerable demands on the accuracy of the computational/theoretical methods for investigating structures and dynamics of complex crystalline molecular system. We have already reported the flipping motion of the phenylene rotator in real time predicted by NCC−DFTB molecular dynamics (MD) simulation [Marahatta *et al*, 2012]. Unfortunately, we did not perform SCC−DFTB molecular dynamics (MD) simulations as it is computationally very expensive.

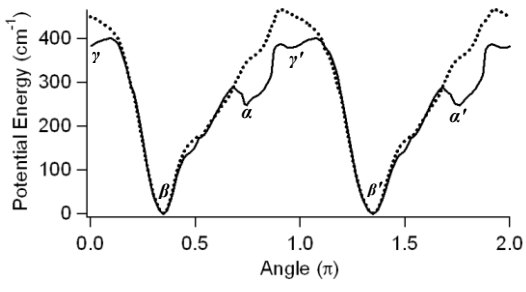

Figure 5: Potential energy as a function of the phenylene dihedral angle under PBC with dispersion energy corrections. The black dotted and thick solid line denote the PESs obtained by the NCC−DFTB and SCC−DFTB respectively. The symbols α, β, and γ stand for three stable positions of the phenylene ring, and α′, β′, and γ′ represent their respective degenerate positions reached by 1 π phenylene flip

IV. CONCLUSIONS

By employing computationally efficient DFTB+ program package, the performances of SCC− and NCC− DFTB methods are examined in reference to the crystalline molecular gyroscope (Figure 1a). We applied both methods to investigate the crystal structures and rotational barriers under periodic boundary condition (PBC) and evaluated their computing abilities. We found that either of these two methods can locate three stable phenylene positions α, β, and γ that are consistent with the three X-ray structures A, B, and C. The theoretically produced three equilibrium structures and the available free volume unit around the phenylene ring present in each of them indicate that the DFTB+ optimizer is as accurate as GAUSSIAN 03 (i.e., the Gaussian external methodology) optimizer. Under periodic boundary condition (PBC), we scanned the potential energy surface (PES) as a function of the dihedral angle between the phenylene ring and a surrounding spoke by both DFTB methods and confirmed the three equilibrium structures A, B, and C (or α, β, and γ) with the respective degenerate positions α', β', and γ' reached by 1 π flip. The predicted activation energy E_a for the flipping from β to γ is lower in NCC−DFTB case. With dispersion energy corrections under PBC, the NCC−DFTB method reproduced only one feature similar to SCC−DFTB derived PES: the most stable structure B, its dihedral angle β and its degenerate position β' reached by 1 π flip. There is no any indication of appearing two more stable positions (α and γ) unlike on the PES derived by SCC-DFTB. Such weak computing ability of NCC-DFTB is also justified by the appearance of slightly higher activation energy E_a for the direct 1 π flip from β to β' position (absence of α and γ' in between β and β' positions) (Figure 5). It is even more unexpected result because the structure B at position β has to flip to position α then to γ' before reaching to β' as observed clearly in X-ray crystallography. These inabilities of NCC-DFTB with dispersion energy parameters under PBC for producing experimentally observed three stable structures elucidate its weak computing performance. This is mostly due to not addressing charge interactions between atoms properly unlike in SCC-DFTB.

Thus, in the complex crystalline molecular gyroscope, the significant van der Waals interactions does exist between the rotating unit and static framework: intra-molecular interactions (and surrounding molecules: inter-molecular interactions) and its proper evaluation is essential while scanning the PES for estimating the rotational barrier. In this work, we have achieved optimum flipping barrier experienced by the rotator by applying SCC-DFTB method with dispersion energy parameters under PBC. It is a strong supporting evidence for the SCC-DFTB method to recommend it for

addressing comparatively weaker hydrogen bonds and van der Waals interactions exist in the molecular crystal. Therefore, the SCC-DFTB with dispersion energy corrections under PBC puts considerable demands on the accuracy of the computational/theoretical methods for investigating structures and dynamics of complex crystalline molecular system.

ACKNOWLEDGEMENT

The authors would like to express their deep gratitude to International Graduate Program for Advanced Science-2007 (IGPAS-2007), Tohoku University and Tohoku development scholarship foundation, Japan for the financial support.

REFERENCES

[1] Aradi, B.; Hourahine, B.; Frauenheim, T. (2007). DFTB+, a Sparse Matrix-Based Implementation of the DFTB Method. Journal of Physical Chemistry A, 111, 5678−5684.
[2] Dominguez, Z.; Dang, H.; Strouse, M. J.; Garcia-Garibay, M. A. (2002). Molecular "Compasses" and "Gyroscopes." III. Dynamics of a Phenylene Rotor and Clathrated Benzene in a Slipping-Gear Crystal Lattice. Journal of American Chemical Society, 124, 7719−7727.
[3] Elstner, M.; Frauenheim, Th.; Kaxiras, E.; Seifert, G.; Suhai, S. (2000). A Self-Consistent Charge Density-Functional Based Tight-Binding Scheme for Large Biomolecules. Physica Status Solidi B, 217, 357−376.
[4] Elstner, M.; Hobza, P.; Frauenheim, Th.; Suhai, S.; Kaxiras, E. (2001). Hydrogen bonding and stacking interactions of nucleic acid base pairs: A density-functional-theory based treatment. The Journal of Chemical Physics 114, 5149−5155.
[5] Elstner, M.; Porezag, D.; Jungnickel, G.; Elsner, J.; Haugk, M.;Frauenheim, T.; Suhai, S.; Seifert, G. (1998). Self-consistent-charge density-functional tight-binding method for simulations of complex materials properties. Physical Review B, 58, 7260−7268.
[6] Frauenheim, T.; Seifert, G.; Elstner, M.; Niehaus, T.; Köhler, C.; Amkreutz, M.; Sternberg, M.; Hajnal, Z.; Di Carlo, A.; Suhai, S. (2002). Atomistic simulations of complex materials: Ground-state and excited-state properties. Journal of Physics Condensed. Matter, 14, 3015−3047.
[7] Frisch, M. J.; Trucks, G. W.; Schlegel, H. B.; Scuseria, G. E.; Robb, M. A.; Cheeseman, J. R.; Montgomery, J. A.; Vreven, T.; Kudin, K. N.; Burant, J. C.; et al. (2004). Gaussian 03, revision E.01; Gaussian, Inc. Wallingford, CT.
[8] Koehler, C.; Hajnal, Z.; Deak, P.; Frauenheim, Th.; Suhai, S. (2001). Theoretical investigation of carbon defects and diffusion in α-quartz. Physical Review B, 64, 085333.
[9] Kohn, W.; Sham, L. (1965). Self-Consistent Equations Including Exchange and Correlation Effects. Physical Review Journal, 140, A1133−A1138.
[10] Marahatta, A. B.; Kanno, M.; Hoki, K.; Setaka, W.; Irle, S.; Kono, H. (2012). Theoretical Investigation of the Structures and Dynamics of Crystalline Molecular Gyroscopes. Journal of Physical Chemistry C, 116, 24845−24854.
[11] Porezag, D.; Frauenheim, Th.; Kohler, T.; Siefert, G.; Kaschner, R. (1995). Construction of tight-binding-like potentials on the basis of density-functional theory: Application to carbon. Physical Review B, 51, 12947−12957.
[12] Rauls, E.; Gutierrez, R.; Elsner, J.; Frauenheim, Th. (1999). Stoichiometric and non-stoichiometric (10$\bar{1}$0) and (11$\bar{2}$0) surfaces in 2H–SiC: a theoretical study. Solid State Communications, 111, 459-464.
[13] Richard, G.J., & Julian, C. (2000). Silicon-Containing Polymers: The Science and Technology of Their Synthesis and Applications. Springer publication, Dordrecht, 186-187.
[14] Seifert, G. (2007). Tight-Binding Density Functional Theory: An Approximate Kohn−Sham DFT Scheme. Journal of Physical Chemistry A, 111, 5609−5613.
[15] Seifert, G.; Porezag, D.; Frauenheim, Th. (1996). Calculations of molecules, clusters, and solids with a simplified LCAO-DFT-LDA scheme. International Journal of Quantum Chemistry, 58, 185−192.
[16] Setaka, W.; Ohmizu, S.; Kabuto, C.; Kira, M. (2007). A Molecular Gyroscope Having Phenylene Rotator Encased in Three-spoke Silicon-based Stator. Chemistry Letter, 36, 1076−1077.
[17] Zheng, G.; Irle, S.; Morokuma, K. (2005). Performance of the DFTB method in comparison to DFT and semiempirical methods for geometries and energies of C20–C86 fullerene isomers. Chemical Physics Letter, 412, 210−216.